Fatigue performance of bonded crack retarders in the presence of cold worked holes and interference-fit fasteners

Syed, A, Zhang, X, Moffatt, J, Maziarz, R, Castelletti, L & Fitzpatrick, M

Original citation & hyperlink:
Syed, A, Zhang, X, Moffatt, J, Maziarz, R, Castelletti, L & Fitzpatrick, M 2017, 'Fatigue performance of bonded crack retarders in the presence of cold worked holes and interference-fit fasteners' *International Journal of Fatigue*, vol 105, pp. 111-118
https://dx.doi.org/10.1016/j.ijfatigue.2017.08.023

DOI 10.1016/j.ijfatigue.2017.08.023
ISSN 0016-7185

Publisher: Elsevier

Fatigue performance of bonded crack retarders in the presence of cold worked holes and interference-fit fasteners

Abdul Khadar Syed[1, 2 *], Xiang Zhang[1], James E Moffatt[2], Robert Maziarz[3], Luigi Castelletti[3], Michael E Fitzpatrick[1]

[1] Faculty of Engineering, Environment and Computing, Coventry University, Priory Street, Coventry CV1 5FB, UK

[2] Materials Engineering, The Open University, Walton Hall, Milton Keynes MK7 6AA, UK

[3]Airframe Research and Technology, Airbus UK, Bristol, BS34 7PA, UK

*Corresponding author; Email address: abdul.syed@coventry.ac.uk (AK Syed), xiang.zhang@coventry.ac.uk (X Zhang), robert.maziarz@airbus.com (R Maziarz), luigi.castelletti@airbus.com (LML Castelletti), michael.fitzpatrick@coventry.ac.uk (ME Fitzpatrick).

Abstract

Bonded crack retarders (BCR) are of particular interest in the aerospace applications for improving fatigue performance of airframe structural assemblies. In respect of structural integrity, a reinforcing strap will require additional fixing by means of riveting or bolting to ensure fail-safety. Cold expansion is currently the common practice of increasing the fatigue performance of fastener holes. Thermal residual stresses introduced during the adhesive curing process at 120°C for strap bonding are of potential concern as they may affect the cold expansion stresses and thereby the fatigue crack growth performance of the fastener hole and reinforced structural assembly. In this paper, Single-Edge-Notched Tension (SENT) specimens are made of aluminium alloy 2624-T351. Fibre metal laminate GLARE is used as BCR strap. SENT specimens with BCR and with BCR plus an interference fit fastener are used to investigate the fatigue crack growth performance. Residual stress was measured by neutron diffraction method on specimens with BCR plus fastener using neutron diffraction. It is found that the GLARE strap provides a 2.3× improvement in life comparing to a plain specimen, and a 1.75× life improvement when a fastener is installed in a cold expanded hole.

Keywords: Bonded crack retarders, Cold expansion, Fatigue crack growth, GLARE, Residual stress

Highlights

- GLARE straps provided significant improvement to fatigue crack growth life.
- Curing residual stress has little effect on cold work induced residual stress field.
- Cold expansion delayed crack remerging from the fastener hole.

1 Introduction

Aircraft structures experience considerable fatigue loading during their service life that imposes significant inspection and maintenance costs for aircraft operators. The primary source of fatigue-based problems is the stress concentrations associated with the numerous assemblies joined by rivets and fasteners. Therefore, the aircraft industry is working towards new design concepts for airframes, maintaining a high level of safety without any weight penalty and/or increase in manufacturing cost. One of the solutions is to use large one-piece integral structures to reduce the number of built-up assemblies. The major concern with integral structures is that they are prone to fatigue cracking owing to single load paths and fewer natural crack stoppers compared to conventional assemblies. As a result, the certification of integral metallic structures is often associated with further safety factor requirements, which leads to additional structural weight and negates the benefit of using integral structures.

To satisfy the damage-tolerance requirements of such structures, technologies have been developed such as selective reinforcement [1] also known as bonded crack retarders [2-4]. The application of bonded crack retarders has proven effective in increasing the fatigue performance of integral metallic structures. These are typically a combination of advanced alloy parts reinforced with highly damage-tolerant materials that are adhesively bonded together. Amongst various bonded crack retarder materials, GLARE fibre-metal laminate has been considered as the best candidate owing to low weight, low thermal residual stresses after bonding at elevated temperature, and excellent fatigue and impact performance [5-10]. Therefore, GLARE was chosen as the crack retarder material for this research.

Despite the benefits of bonded crack retarders, secondary bending and thermal residual stresses are two concerns. Secondary bending is a consequence of the single-sided strap bonding process and this can affect the fatigue performance of the reinforced

structure. Whilst secondary bending can be reduced by double-sided strap bonding, this is unlikely to be deployed in aircraft manufacture owing to the aerodynamic requirements of the exterior surface of the reinforced structure.

The use of adhesive instead of rivets or bolts to join substrate and reinforcements allows full exploitation of the benefit of integral structures. However, adhesively bonded straps require an additional means of fixing, either by rivets or fasteners, to ensure structural fail-safety in the event of complete disbond. Such fixings require drilling holes that introduce stress concentration. The stress concentrations can be reduced and the fatigue performance of fastener holes can be enhanced by the cold expansion process [11]. Fatigue crack growth performance of a reinforced structure that contains cold expansion stresses and a fastener has not been investigated prior to this research.

In addition, drilling fastener holes through the reinforced structure can damage the GLARE and the adhesive bonding interface. Typical damage mechanisms that can occur are push-out or peel-up delamination, fibre-matrix debonding, and interlaminar cracking. Experimental tests and FE analyses performed in [12] revealed that drilling also leads to hole-edge quality issues, resulting in edge chipping and glass fibre damage. Such damage is highly undesirable, and can lead to delamination and the loss of mechanical strength and stiffness of the strap and reinforced structure.

To the authors' knowledge there is no previous work investigating the fatigue crack growth performance of aluminium 2624-T351 reinforced by bonded GLARE straps in the presence of a cold expanded hole with interference fit fastener. This study aims at investigating the potential of the bonded crack retarder concept in structural assemblies that have fasteners to ensure fail-safety with the intention of proving the technology for inclusion of integrally machined structures reinforced with bonded crack retarder in future aircraft designs. The focus is on the effect of the crack retarder in the presence of a fastener.

2 Materials and test specimen

Aluminium alloy 2624-T351 was used as the substrate material and fibre metal laminate GLARE 6/5 was chosen as the strap. The GLARE strap consists of six AA2024-T3 alloy sheets (0.4 mm thick) with five intermediate prepreg layers of unidirectional glass fibre-reinforced epoxy (0.26 mm thick) oriented along the longitudinal direction of the

strap (X-axis, Fig 1a. The geometry of the specimen with a strap is shown in Fig 1a and the actual cross-section of the specimen is presented in Fig 1b. Initial crack orientation is perpendicular to the rolling direction of the substrate. This orientation is determined by the application requirement. The thickness of the substrate and strap is 5.0 mm and 3.7 mm respectively. Mechanical properties of the substrate and strap are listed in Table 1. Before the strap bonding process, a 17 mm notch was machined in the substrate to act as a crack starter for the fatigue crack growth testing. The specimen configuration is shown in Fig 1.

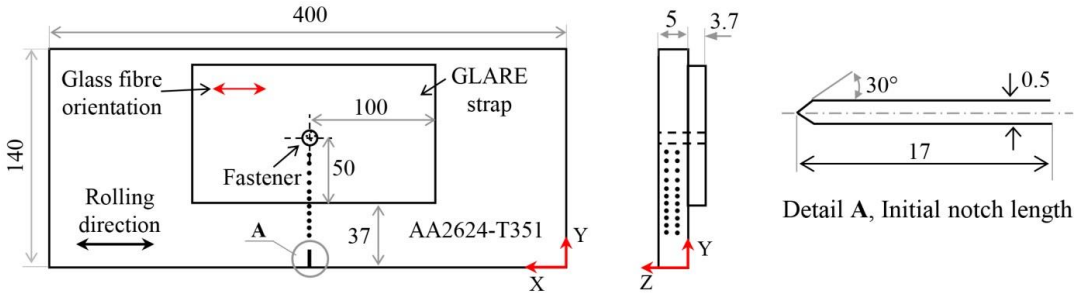

(a) Geometry and dimension of SENT specimens reinforced with a GLARE strap (unit : mm and not to scale), dotted lines shows residual stress measurement line. Fastener in the middle of the strap.

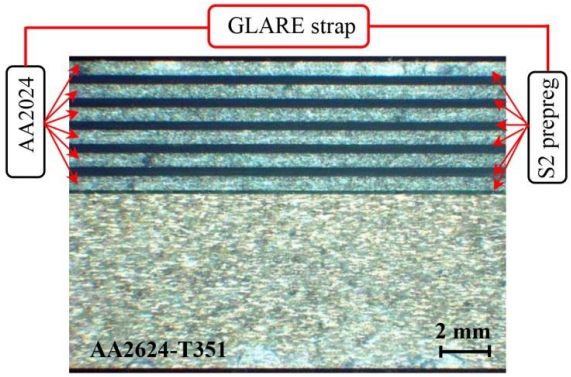

(b) cross sectional view of the specimen used for investigation

Fig 1: (a) Schematic of the SEN(T) specimen, (b) cross-sectional view of the substrate and GLARE strap.

One important parameter that contributes to the performance of the BCR is the global stiffness ratio μ, which is defined as:

$$\mu = \frac{\sum(E_{strap} \cdot A_{strap})}{(E_{Al} \cdot A_{Al}) + \sum(E_{strap} \cdot A_{strap})} \quad (1)$$

where E_{strap}, E_{Al} and A_{strap}, A_{Al} are the elastic modulus and cross-sectional area of the straps and the substrate material respectively. In this study, a global stiffness ratio of 0.32 was chosen.

Table 1: Mechanical properties of substrate and GLARE strap (laminate)

Material	**AA2624-T351** [13]	**Glare 6/5**
Young's modulus E_{11} (GPa)	71	64
Tensile strength σ_{TS} (MPa)	448	1091
Yield strength, σ_{ys} (MPa)	331	340
Fracture toughness, K_{IC} (MPa$\sqrt{m}$)	53	-

The surface of the substrate and the external aluminium sheets of the GLARE were etched with Phosphoric Acid Anodizing (PAA), which involves alkaline degreasing followed by PAA and priming with BR 127, a modified epoxy phenolic primer with corrosion inhibiting properties [14, 15]. The substrate and strap assembly was bonded using FM 94 [16], a high-temperature (120°C) curing adhesive. The curing process is described below.

- Apply vacuum at ambient temperature for a minimum of 15 minutes and increase the temperature at a rate of 3°C/min from ambient to 125 ± 5°C, and increase pressure in autoclave to 520 kPa.
- Vent vacuum when the pressure reached 415 kPa, or when the temperature reached 60°C, then apply a pressure of 520 kPa at 125°C for 90 minutes.
- After 90 minutes, turn off the heat and allow cooling to below 60°C, whilst maintaining the pressure, prior to removing the samples from the autoclave.

To check the bond quality, specimens were inspected using an ultrasonic phased array device Olympus Omniscan Mx with a 5L64-I1 probe. A rolling wheel encoder was added to the probe in order to measure the scanning distance. The resolution of the encoder was 12 steps/mm.

After bonding, an interference fit fastener was installed through the thickness of the assembly. The interference fit fastener hole was 3% cold expanded using the FTI split-sleeve cold expansion and the final diameter of the fastener hole was 6.35 mm. During this procedure, the mandrel was pulled from the non-reinforced side (entry face) towards the reinforced side (exit face).

3 Experimental procedure

3.1 Grain size and texture measurements

The substrate material used in this investigation is formed by rolling; a strong preferred grain orientation will be developed in the specimen. When the material passes through the rollers, the interaction with the roll affects the homogeneity and grain size in three dimensions. Therefore, grain size measurements were performed in the rolling (X), transverse (Y) and normal (Z) directions. For this, three samples were extracted from the substrate, mounted, ground, polished, and etched with Keller's Reagent for 12 seconds.

3.2 Measurement of out-of-plane deformation

The specimens were subjected to in-plane loading in fatigue testing with loading along the material longitudinal direction (the X-direction, see Fig1). Owing to the asymmetric strap configuration (straps were bonded on one side of the plate only), out-of-plane deformation occurred after the curing of the straps, and additionally during the fatigue loading because of the secondary bending effect (see Fig 3).

Following curing of the crack retarders at elevated temperature, residual stresses exist owing to the mismatch of the coefficient of thermal expansion between the aluminium substrate and the GLARE straps. Because of the asymmetric strap configuration, these residual stresses will cause out-of-plane deformation. This deflection was measured on the specimens after the strap bonding process using a coordinate measurement machine. The measurement was performed on the unreinforced (back) side along the specimen longitudinal direction (X) with a 1 mm measurement interval.

3.3 Residual stress measurements

Residual stress measurements were performed using neutron diffraction using the ENGIN-X instrument at the ISIS neutron source, UK; and the SALSA instrument at the ILL, France. Neutron diffraction is a non-destructive technique to measure strains and thereby stresses within metallic structures. The principle of residual stress measurements using neutron diffraction is to determine the change in lattice spacing between the measurement points, relative to a stress-free value. The average lattice

strain within the gauge volume for a given direction for particular crystallographic planes can be calculated using:

$$\varepsilon = \frac{d_{hkl} - d_{0,hkl}}{d_{0,hkl}} \quad (2)$$

Where ε_{hkl} is the strain, d_{hkl} is the lattice plane spacing and $d_{0,hkl}$ is the stress-free lattice parameter of the material. The stresses are then calculated by using the triaxial form of Hooke's law:

$$\sigma_{ii} = E_{hkl} \frac{(1 - \upsilon_{hkl})\varepsilon_{ii,hkl} + \upsilon_{hkl}(\varepsilon_{jj,hkl} - \varepsilon_{kk,hkl})}{(1 + \upsilon_{hkl})(1 - 2\upsilon_{hkl})} \quad (3)$$

Where *i*, *j*, *k* are orthogonal directions.

ENGIN-X is a time-of-flight diffractometer where multiple reflections can be measured simultaneously. ENGIN-X Script Based Analysis (EX-SBA) was used for the data analysis where Pawley refinement was used to determine the lattice parameters: this has been shown to yield a good approximation of the engineering strain in a material [17, 18].

SALSA is a monochromatic diffractometer [19] and the wavelength of the neutron beam used for residual stress measurements was 1.648 Å. The data obtained were analysed using the Large Array Manipulation Program (LAMP). The chosen wavelength of the neutron beam is selected for the material being investigated is based on the measured lattice plane. In this research, the specimens were made of aluminium which is face-centred cubic (FCC) and the {311} lattice plane was chosen for the residual stress measurements because of its high multiplicity factor (24 for {311}), and because the elastic response of the 311 plane closely reflects the macroscopic elastic response of aluminium.

Residual stress measurements were performed in three orthogonal directions and at two different thickness locations, at *z* =1.5 and 3.5 mm from the reinforced side in the aluminium plate (Fig. 1). Residuals tress measurements at *z* = 1.5 mm were performed at ENGIN-X, UK and at *z* = 3.5 mm were performed at SALSA, France. All the measurements at ENGIN-X and SALSA were performed with a gauge volume of 2 × 2 × 2 mm^3. Stress-free reference measurements were performed in all three measured directions (hoop, radial and axial with respect to the fastener hole) to account for any texture and plastic anisotropy in the material and the respective stress-free reference will be used in computation of residual stresses. Stress-free measurements were performed

from a point close to an edge of the substrate well outside of the bonding region at the same positions through the plate thickness.

3.4 Fatigue crack growth testing

Fatigue crack growth testing was performed at room temperature using a 100 kN MTS servo-hydraulic test machine and constant amplitude load with a maximum stress of 60 MPa at 10 Hz and with a load ratio, *R* of 0.1. Tests were performed according to ASTM E647. Crack length measurements were performed optically by using a travelling microscope with an accuracy of ±0.01 mm. For specimens with a strap, crack length measurements were performed on the non-reinforced side of the specimen. A total of nine specimens were tested, three for each case of: without a strap, with a strap, and with a strap and interference fit fastener fitted into the cold expanded hole.

4 Results and discussion

4.1 Grain size and texture measurements

AA2624-T351 alloy is typically solution-heat-treated and naturally-aged. Fig 2 shows a three-dimensional image of the grain distribution structure. The grain structure is a "pancake" structure. Grain size measurements were performed using ASTM E112. In the rolling direction, the grain size was found to be 113-134 μm, in the transverse direction 33-40 μm, and in the normal direction 28-33 μm. As expected, rolling significantly affected the grain size in the rolling direction and it is likely that there will be resulting in intergranular stresses leads to diffraction peak broadening influencing the strain measurements hence residual stresses.

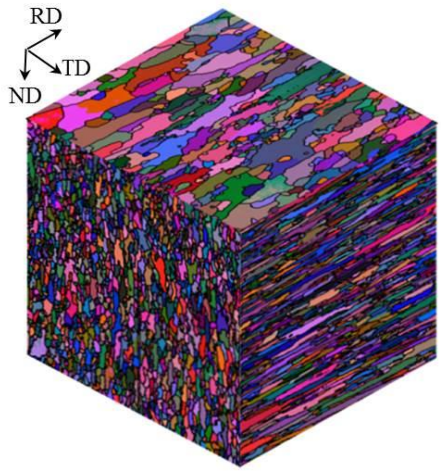

Fig 2: Three-dimensional image of grain distribution in AA2624-T351 (RD-rolling direction, TD-transverse direction, and ND-normal direction)

Furthermore, elastic anisotropy resulting from rolling will give rise to different strains in different crystallographic planes in grains aligned along the rolling direction. To minimise the influence of elastic anisotropy, it is recommended that appropriate diffraction elastic constants should be used to determine the residual stresses [20]. This approach is used in the residual stress measurements of this research where respective stress-free and elastic modulus is used to compute the residual stresses.

4.2 Measurement of out-of-plane deformation

Fig 3a shows a schematic of the specimen deformation before and after the strap bonding process. Fig 3b shows the measured out-of-plane deformation resulting from the bonding process. The maximum deformation is 0.9 mm, which is 18% of the substrate thickness.

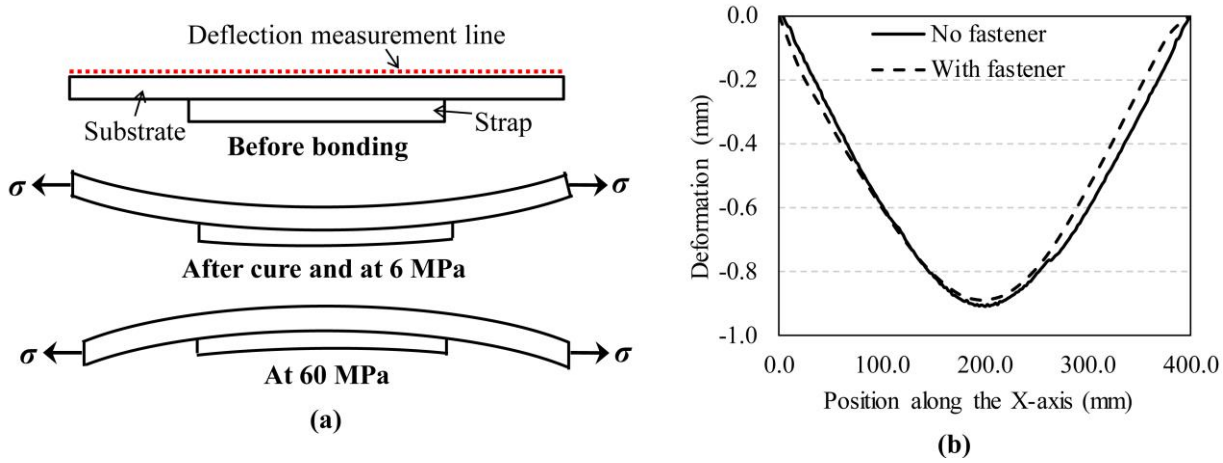

Fig 3. (a) Sketch of specimen deformation before and after strap bonding, and at the maximum and minimum applied cyclic stresses, (b) Measured out-of-plane deformation of the SEN(T) specimen after bonding the GLARE strap.

After strap bonding, with no external load, specimen deformation results in compressive [21] and tensile stresses on the unreinforced and reinforced sides respectively. Owing to the geometric asymmetry, the out-of-plane deformation will change when the specimen is under uniaxial loading. The change in deformation shape during fatigue loading is depicted in Fig 3a. It should be noted that the deformation observed at the minimum applied stress 6 MPa is virtually the same as no applied load caused predominantly by the mismatch of the coefficients of thermal expansion. However, at the maximum applied stress of 60 MPa, the deformation is reversed, giving tensile stresses on the unreinforced side that accelerate fatigue crack growth on that side. Previous research

that investigated the behaviour of middle-crack tension (M(T)) specimens reinforced with GLARE bonded crack retarders also found that the specimen deformation significantly changed during the fatigue loading [9].

4.3 Residual stress measurements

High-temperature adhesive curing results in the development of thermal residual stresses; and the impact of residual stresses are of particular interest. Residual stress measurements were performed along the crack growth direction (Y-direction) at z = 1.5 mm and 3.5 mm thickness locations as shown in Fig 1. Owing to time constraints, measurements at z = 1.5 mm were performed at ENGIN-X and at z = 3.5 mm were performed at SALSA. The results are presented in Fig 4.

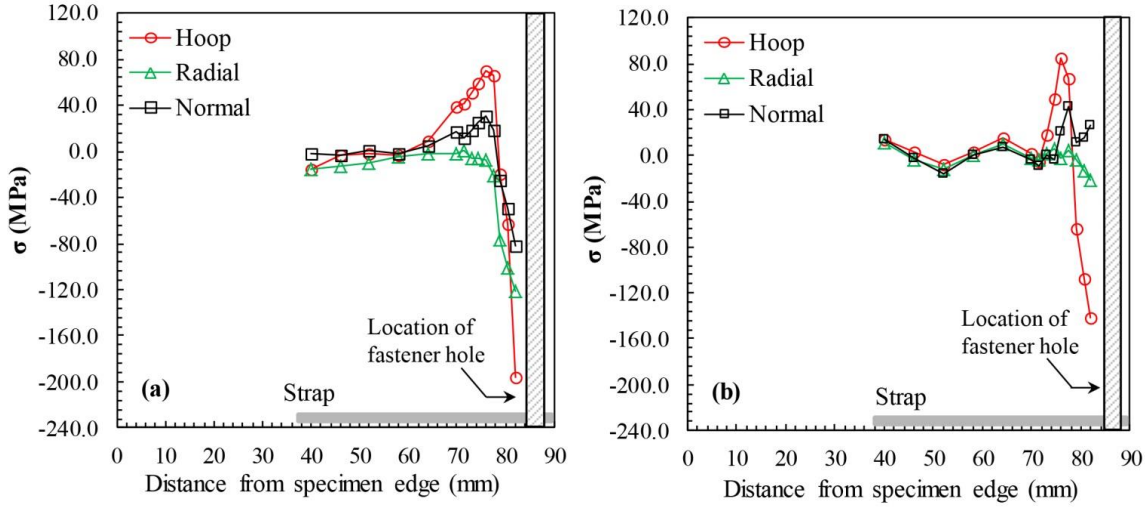

Fig 4: Residual stresses in the aluminium plate at (a) z = 1.5 mm and (b) z = 3.5 mm from the reinforced side, showing the combined effects of the strap and hole cold expansion. No applied load was present.

Residual stress measurements performed prior to interference fit fastener reveals that the strap bonding on to the substrate resulted in low, if any, residual stresses in the substrate, within the sensitivity of the measurement technique. In addition, measurements performed under the strap show a small scatter in the data, particularly at z = 3.5 mm, that is partly because the hydrogen-containing epoxy present in the assembly causes incoherent scattering of the neutrons which impairs the signal-to-noise ratio. In addition, measurements (at z = 3.5 mm) performed at SALSA used only a single diffraction peak which will be sensitive to changes in texture and hence intergranular stress through the plate thickness. However, this is not the case for the

measurements performed at ENGIN-X, where Pawley refinement of many diffraction peaks was used which effectively removes any texture effects.

Towards the fastener hole, compressive stresses are measured for both the hoop and radial components that are a result of the cold expansion process. Compressive residual stresses persist up to 5 mm from the edge of the hole. Cold expansion results in a non-uniform stress distribution through the thickness of the specimen, with the values of residual stresses being higher on the exit face (z = 1.5) of the mandrel compared to the entry face (z = 3.5). Compressive residual stresses are balanced by tensile residual stresses away from the hole with maxima of about 80 MPa.

4.4 Fatigue crack growth testing

Fig 5 shows the results of constant amplitude load fatigue crack growth tests on all specimens, three of each case. Fig 5a shows that application of the strap resulted in significant life improvement compared to the specimens without a strap, confirming the efficacy of the bonded crack retarder concept. Table 2 shows summary of fatigue crack growth test results. The strap gave a 2.3× fatigue life improvement compared to specimens without strap. The specimens with a strap and a fastener have a longer life compared to specimens without a strap, but a shorter life than without the fastener in place.

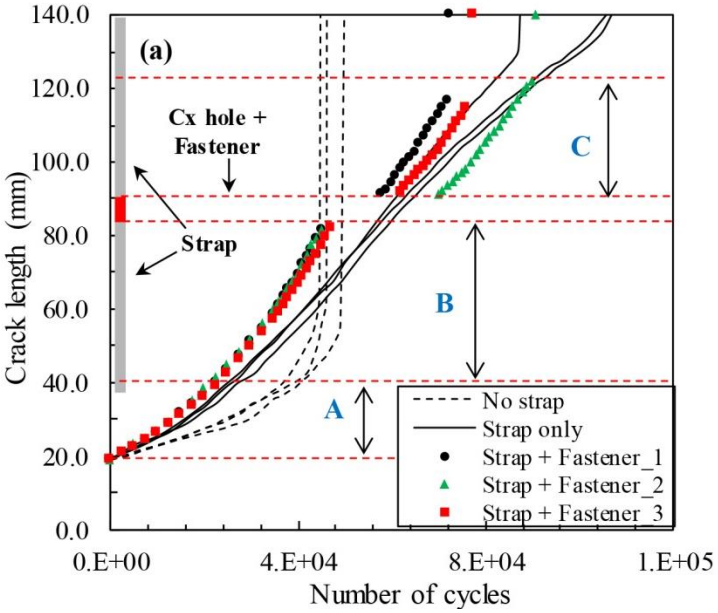

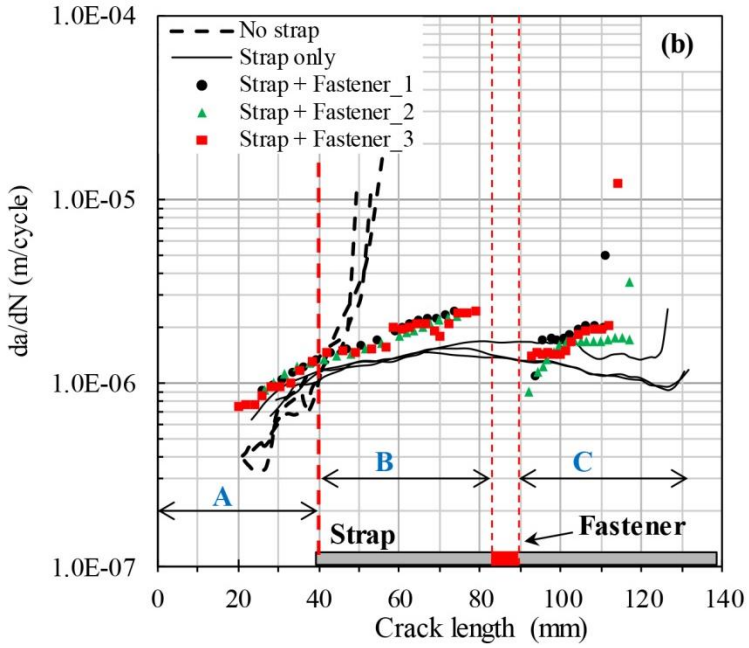

Fig 5: (a) Measured crack length vs number of cycles, (b) crack growth rate vs. crack length for AA2624-T351 for three cases of without strap, with strap, and with strap plus a fastener. Three tests were performed for each case. Region **A** shows crack growth acceleration for the "with strap" and "with strap plus fastener" cases. Region **B** and **C** show crack bridging effect and faster crack growth rate for the "with strap plus fastener" compared to "with strap" case.

In region A on Fig 5, specimens with straps show crack growth acceleration owing to the effect of the secondary bending stress (Fig 3a) which is high on the unstrapped side. In region B, further acceleration occurs owing to the balancing tensile stresses away from the cold worked hole. Fig. 4 shows that the balancing tensile residual stress (hoop stress component) is as high as 80 MPa. Therefore, before the crack reached the fastener hole, it was in the tensile residual stress field resulting in an accelerated crack growth rate. Crack growth acceleration happened in the crack length range of 53-82 mm, corresponding well with the measured tensile residual stress zone. This acceleration can be seen more clearly on Fig 5b: the slope of da/dN is increased in the tensile residual stress zone, but the overall da/dN is reduced because strap bridging is also present. In region C, the strap crack bridging and cold work compressive stress interact, resulting in overall retardation. Because of the balancing tensile stresses in region B, the overall fatigue life of the fastener specimen is shorter than that with strap only.

Table 2: Summary of fatigue crack growth test results

	Number of cycles to failure			
	Test 1	**Test 2**	**Test 3**	**Average**
No strap	46114	44751	49830	46898
With strap	106894	105754	87347	87347
With strap plus fastener	72406	90946	77371	77371

Fig 5b shows crack growth rate as a function of crack length. Specimens with a strap plus fastener exhibit interesting fatigue crack growth behaviour, as the number of cycles to failure was noticeably different for each specimen tested. The number of cycles required for the crack to reach the fastener (84.2 mm crack length) was approximately the same for all the specimens. Specimen 2 shows ~20% higher fatigue life compared to specimens 1 and 3. The difference in life of the three specimens is in region C, which may be owing to the crack closure effect when exiting the hole as the compressive residual stress is nearly 160–200 MPa. Close observation of the specimens after failure reveals that the shorter fatigue life of specimen 1 and 3 is linked to the crack path. Fig 6 shows images of the crack path in the specimens reinforced with a strap and fitted with a fastener. For specimen 2, the crack entered the hole at the hole centreline where maximum compressive stress (hoop stress component) is present (Fig 4). This greatly slows the crack growth rate, requiring a greater number of cycles to pass through the compressive stress field to the hole edge, and then to reinitiate a crack from the exit side. For specimens 1 and 3, the crack passed to the upper side of the fastener hole where the cold expansion residual compressive residual stresses are not as effective, therefore requiring fewer cycles for the crack to reach the hole edge and then reinitiate a crack from the exit site. Consequently, specimen 2 showed greater fatigue life compared to specimens 1 and 3; and the number of cycles required for the crack to leave the fastener is different: 13000, 25000, and 15000 cycles for specimen 1, 2 and 3 respectively.

Once the crack reaches the strap, the crack bridging effect significantly reduces the crack growth acceleration (crack length greater than 37 mm), demonstrating the significant benefit of the BCR.

4.5 Strap delamination and fracture surfaces

An important parameter determining the retardation effectiveness of the bonded crack retarders is the strap delamination behaviour during fatigue. The two possible strap delamination processes are: (i) delamination between the substrate and strap interface (crack propagation through the adhesive); and (ii) delamination within the strap (crack propagation through the first epoxy layer of the strap) [9]. In this research, all the reinforced specimens showed the first type of failure, with the crack advancing through the FM94 adhesive, as shown in Fig 7. The delamination onset is dependent on several parameters such as the stress concentration at the substrate and adhesive interface, secondary bending, and the residual stresses present. The delamination front is roughly triangular.

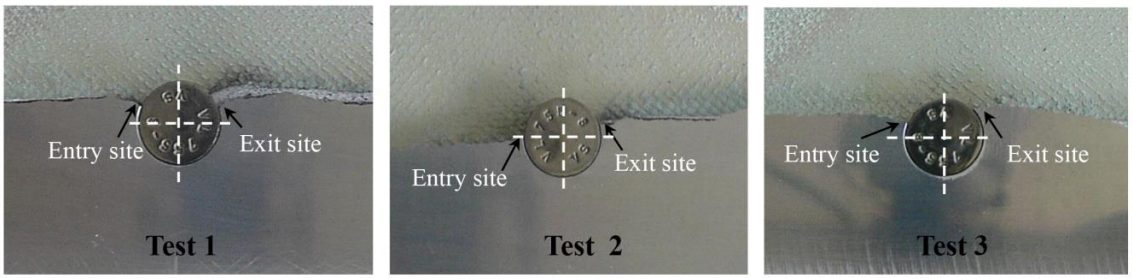

Fig 6. Crack path close to the fasteners in specimens reinforced with strap and fitted with a fastener.

Close examination of the fracture surface revealed features that are presented in Fig 8. The fracture surface observed at location 1 (see Fig 8, at 35 mm from the EDM notch root) which is under the strap shows fatigue surface with poor visibility of striation marks compared to location 3. The fracture surface at location 1 also appears rough compared to other locations. This might be attributed to the reduction in crack growth rate (Fig. 5) owing to the strap's crack bridging effect and crack closure. The fracture surface at location 2 on the edge of the fastener hole showed small microvoids similar to the fast fracture surface. Once the crack propagates through the compressive stresses, the fracture surface away from the fastener appears smooth with clear striation marks. The smooth surface is due to the increase in fatigue crack growth rate and reduction in strap retardation. Furthermore, at location 2 there is no evidence of the striation marks which are visible at locations 1 and 3. Fracture surface at location 3 is smoother than location 1. This might be due to increase in crack growth rate that can observed from

Fig. 5 and less crack bridging and crack closure compared to location 1. Location 3 fracture surface shows clear striation marks that were difficult to observe in location 1. Finally, the fracture surface at location 4 shows microvoids, confirming the fast fracture phase.

4.6 GLARE interface damage

As composites are non-homogeneous and anisotropic, hole drilling raises specific problems that might affect component strength and fatigue life. Damage and delamination induced in the glass fibre layers of the GLARE due to drilling were inspected by SEM.

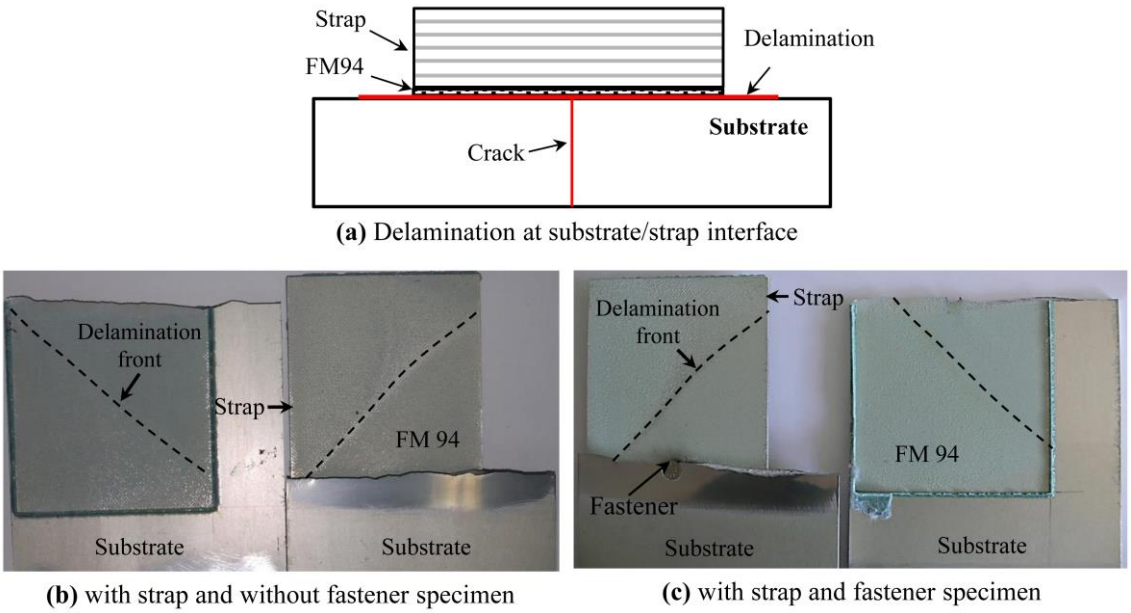

Fig 7: Post failure specimens showing cohesive failure and triangular delamination front (a) with strap (b) with strap and fastener, test 2

Fig 9 shows an SEM image of the drilled and cold-worked GLARE strap layers. It is apparent that drilling a hole through the GLARE strap has resulted in noticeable fibre loss in the GFRP layers within the GLARE strap. This occurs because when the drill moves inwards it creates a peeling effect from the material surface that can cause a small amount of material loss within the adhesive layers. We did not find any evidence of inter-laminar cracking, fibre/matrix delamination orpush-out delamination of the aluminium layers that might have resulted from the drilling process.

Conclusions

The efficacy of the GLARE bonded crack retarders in a simulated airframe configuration was investigated by performing constant-amplitude-load fatigue crack growth tests on SEN(T) specimens reinforced with a wide GLARE strap. The strap was bonded to one side of the substrate only, as would be the case in the majority of target applications. A fastener was installed through the strap and substrate in cold expanded hole. The following conclusions are drawn.

1) The single-sided strap bonding and elevated temperature adhesive cure caused out-of-plane deformation owing to the mismatch of the coefficients of thermal expansion between the strap and substrate.
2) The cold expansion process produced desirable compressive residual stresses around the fastener hole between –150 and –200 MPa, being higher on the exit face of the expansion mandrel. This has effectively delayed crack re-emerging from the hole. When the crack path was directed towards the hole centre, the longest fatigue life was achieved.
3) The specimen with a strap showed a 2.3× fatigue life improvement and the specimen with a strap plus fastener showed a 1.7× fatigue life improvement compared to the baseline specimens without a strap, confirming the efficacy of the bonded crack retarder concept. The reduced fatigue life improvement in the fastener case is owing to the balancing tensile residual stresses away from the cold worked fastener hole that is on the crack path. The life of the samples containing a fastener showed some dependence on the crack path in relation to the cold worked hole.
4) Cohesive delamination of the adhesive was observed at the substrate and strap interface as the crack in substrate passed under the strap.

As a result of this study, it is recommended that, if discrete/selective fasteners are used to safeguard the bonded straps, it should be avoided having cold worked holes and fasteners arranged on the potential path of fatigue cracks. If the likely crack path is known, any fastener holes should be offset from the crack path.

Acknowledgements

Shu Yan Zhang and Saurabh Kabra at Engin-X, ISIS neutron source facility, UK and Thilo Pirling at SALSA, Institut Laue-Langevin, France are greatly acknowledged for

their support during the residual stress measurements. The authors would like to thank all the participants involved in this project including Alcoa, and Canfield University. MEF is grateful for funding from the Lloyd's Register Foundation, a charitable foundation helping to protect life and property by supporting engineering-related education, public engagement and the application of research.

References

[1] Garratt M, Heinimann M, Bucci R, Kulak M. Improving damage tolerance of aircraft structures through the use of selective reinforcement. 23rd Symp. Int. Comm. Aeronaut. fatigue, 2005, 197–208.

[2] Zhang X, Irving P, Boscolo M, Allegri G, Figueroa-Gordon D. Improving fail-safety of aircraft integral structures through the use of bonded crack retarders. 24th Symp. Int. Comm. Aeronaut. Fatigue, Naples, Italy: 2007.

[3] Zhang X, Boscolo M, Figueroa-Gordon D, Allegri G, Irving PE. Fail-safe design of integral metallic aircraft structures reinforced by bonded crack retarders. Eng Fract Mech 2009;76:114–133.

[4] Irving PE, Zhang X, Doucet J, Figueroa-Gordon D, Boscolo M, Heinimann M, et al. Life extension techniques for aircraft structures – extending durability and promoting damage tolerance through bonded crack retarders ICAF 2011 structural integrity: influence of efficiency and green imperatives. In: Komorowski J, editor., Springer Netherlands; 2011: 753–770.

[5] Liljedahl CDM, Fitzpatrick ME, Edwards L. Distortion and residual stresses in structures reinforced with titanium straps for improved damage tolerance. Mater Sci Eng A 2008;486:104–111.

[6] Syed AK, Fitzpatrick ME, Moffatt JE. Effect of Thermal Residual Stresses on Bonded Structures Containing Cold Expanded and Bolted Holes. Adv. Mater. Res.2014; 996: 682–687.

[7] Syed AK, Fitzpatrick ME, Moffatt JE. Evolution of residual stress during fatigue crack growth in an aluminium specimen with a bonded crack retarder. Compos Struct 2014;117:12–16.

[8] Syed AK, Fitzpatrick ME, Moffatt JE, Doucet J, Durazo-Cardenas I. Effect of impact damage on fatigue performance of structures reinforced with GLARE bonded crack retarders. Int J Fatigue 2015;80:231–137.

[9] Syed AK, Zhang X, Moffatt JE, Fitzpatrick ME. Effect of temperature and thermal cycling on fatigue crack growth in aluminium reinforced with GLARE bonded crack retarders. Int J Fatigue 2017;98:53–61.

[10] Syed AK, Fitzpatrick ME, Moffatt JE. Residual stresses in aerospace structures reinforced with bonded crack retarders. J Strain Anal Eng Des 2016;51:170–175.

[11] Zhang X, Wang Z. Fatigue life improvement in fatigue-aged fastener holes using the cold expansion technique. Int J Fatigue 2003;25:1249–1257.

[12] Giasin K, Ayvar-Soberanis S, French T, Phadnis V. 3D Finite Element Modelling of Cutting Forces in Drilling Fibre Metal Laminates and Experimental Hole Quality Analysis. Appl Compos Mater 2016:1–25.

[13] https://www.alcoa.com/mill_products/catalog/pdf/AAP2624-factsheet.pdf, Accessed on 1st August 2016.

[14] Park SY, Choi WJ, Choi HS, Kwon H, Kim SH. Recent Trends in Surface Treatment Technologies for Airframe Adhesive Bonding Processing: A Review (1995–2008). J Adhes 2010;86:192–221.

[15] Wu G, Yang J. The mechanical behavior of GLARE laminates for aircraft structures. JOM J Miner Met Mater Soc 2005;57:72–79.

[16] https://www.cytec.com/sites/default/files/datasheets/FM_94982015.pdf . Accessed February 2, 2017.

[17] Santisteban JR, Daymond MR, James JA, Edwards L. ENGIN-X: a third-generation neutron strain scanner. J Appl Crystallogr 2006;39:812–825.

[18] Daymond MR, Bourke MAM, Von Dreele RB, Clausen B, Lorentzen T. Use of Rietveld refinement for elastic macrostrain determination and for evaluation of plastic strain history from diffraction spectra. J Appl Phys 1997;82(4):1554-1562.

[19] Pirling T, Bruno G, Withers PJ. SALSA—A new instrument for strain imaging in engineering materials and components. Mater Sci Eng A 2006;437:139–144.

[20] Fitzpatrick, ME, Lodini A. Analysis of Residual Stress by Diffraction using Neutron and Synchrotron Radiation. CRC Press; 2003.

[21] Okafor C, Singh N, Enemuoh UE, Rao SV. Design, analysis and performance of adhesively bonded composite patch repair of cracked aluminum aircraft panels. Compos Struct 2005;71:258–270.